Multi-Modal System for the Characterization of Photovoltaic Structures

R. Ciocan[1], B. H. Hamadani[2], S. Seyedmohammadi[3], D. Assalone[1], Z. Li[1], E. Manke[1], M. Carroll[4], E. Ciocan[5], M. Hudait[6], O. Thériault[7], K. Hinzer[7], M. Slocum[8], A. Maros[8], C. Kerestes[8] and S. Hubbard[8]

[1]Oriel Instruments, Newport Corporation, Stratford, CT, USA, [2] Engineering Laboratory, National Institute of Standards and Technology, Gaithersburg, MD, USA, [3]Ferro Corp, Vista, CA, USA, [4]RFMD, Greensboro, NC, USA, [5]Wentworth Institute of Technology, Boston, MA USA, [6]Virginia Tech, Blacksburg, VA, USA, [7]SUNLab, University of Ottawa, Ottawa, Canada, [8]Rochester Institute of Technology, Rochester, NY, USA

***Abstract* — This study shows the results obtained with an integrated system capable of performing the main modalities used in photovoltaic (PV) device characterization: current-voltage (I-V), spectral response characterization, reflectance measurements and electroluminescence measurements. The system is able to provide scanning maps of the PV parameters for the device under test such as: external quantum efficiency (EQE), internal quantum efficiency (IQE), and maximum power. I-V curves can be obtained under monochromatic or white light in the same location where the IQE curves are measured without a supplemental repositioning of the device under test. The results shown in this study demonstrate that this system can provide a spectral resolution better than 2 nm. For IQE measurements both diffusive and specular components of reflectance can be determined. Electroluminescence (EL) Spectroscopy measurements at different applied voltages are presented.**

***Index Terms* — spectral characterization, electroluminescence spectroscopy, charge carrier lifetime, photovoltaic cells, silicon.**

I. Introduction

Various photovoltaic research groups were measuring the cell QE in the 1970s and earlier if one includes the measurements on detectors only. The first system capable of measuring the absolute external quantum efficiency (QE) based on a beam splitter was proposed by Say and collaborators in 1977 [1]. Metzdorf's paper [2] describes the first really low noise, high accuracy QE system suitable for PV calibrations. Metzdorf's system was based on a dual beam splitter. Our method described in this study is a direct continuation of the work presented in [1] and [2] but instead of using a dual beam splitter we use a three- way beam splitter. There are several systems in the market that can perform QE measurements. These systems also measure the reflected component based on the integrating sphere system, a method that is described in United States Patent 5757474 [4]. Zalewski [5] showed in 1988 in a special NIST publication that it was possible to get part of the diffusive component of the reflected signal using a detector placed normally to the sample. Based on experience accumulated in more than 20 years in spectral characterization of photovoltaic devices, a set of requirements [3] has been established. Some of those requirements have been incorporated in the ASTM 1021 and ASTM 2236 standards that regulate the spectral characterization of photovoltaic devices. The system that we present in this work meets all the requirements of this standard and exceeds the requirements of this standard by performing I-V measurements for each wavelength, and by providing the possibility of investigating the temperature dependence [3] of external quantum efficiency QE, internal quantum efficiency, IQE, and short circuit current, Isc. The system has the capability of providing the spatial distribution of all these quantities – which also exceeds the standard requirements.

II. System Description and Characterisation

The key element of the system is a four-channel multiplexer that allows quasi simultaneous data acquisition from 3 photo detectors and from the photovoltaic device under test. The monochromatic light from a tunable optical source is delivered via a three- way beam splitter simultaneously to the sample and to a reference detector (Figure 1). The three way configuration also allows measuring the light reflected by the sample. The external and internal QE are measured simultaneously. A dedicated software program on a laptop computer controls the power supply, the monochromator, the lock-in amplifier, the multiplexer and the trans-impedance amplifier all at the same time

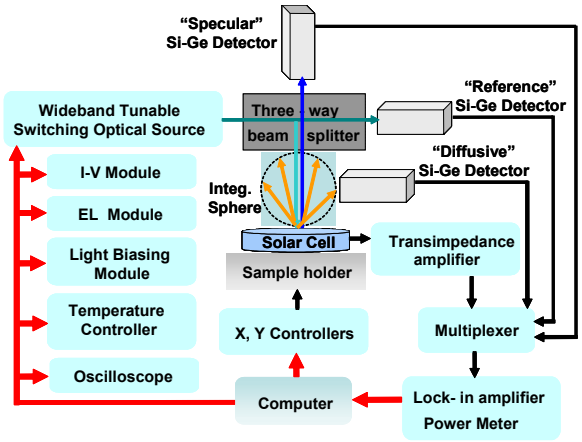

Figure 1 Block diagram of the setup used in this work.

The computer controlled trans-impedance amplifier maintains the sample at zero voltage. The short circuit current

is saved for each measurement. The trans-impedance amplifier is not only a traditional amplifier but, being an instrument fully controlled by computer, it is able to provide the AC and DC components of the signal coming from the sample, control the gain, control the level and polarity of voltage biasing and the level of light biasing. An oscilloscope coupled to the AC output of the trans-impedance amplifier is used to acquire signals needed for decay time measurements. The oscilloscope was found to be very useful in checking for possible ripples or for clipping [3] of the signal fed to the lock-in amplifier. At the initial stage of this study both pyroelectric and Si/Ge detectors were considered. The dark current for pyroelectric detectors was found to be 2 orders of magnitude higher than that for Si/Ge detectors. Therefore Si/Ge detectors have been used exclusively in applications that requires high signal to noise ratio.

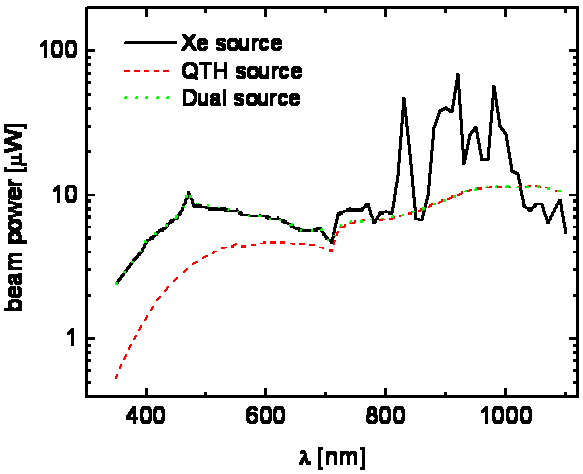

Figure 2 Typical output for the dual switching optical source

The system used in this study can perform the following procedures on the photovoltaic device under investigation without moving it: 1) spectral response characterization; 2) measuring the current - voltage (I–V) curve for monochromatic or light bias; 3) measuring the specular and diffuse component of reflectance; 4) EL investigation. In addition to local investigation, the system is instrumented with X-Y stages allowing the mapping of the main quantities of interest (i.e. QE, IQE, Pmax). The light source used in the spectral characterization is either a xenon lamp or a quartz tungsten halogen (QTH) lamp. The system has the capability for automated switching between the light sources during spectral characterization. This switching between light sources was first introduced at the system currently used at the National Institute of Standards and Technology (NIST).

The NIST spectral response measurement system consists of a triple grating monochromator (presently, 300 nm to 1800 nm spectral range) with a custom dual light source set up for monochromator light input and electronic instruments designed to measure small ac photogenerated signals. The light bias is set up to illuminate the entire active area of the device (overfilled illumination) and the current trans-impedance amplifier used to measure and amplify the chopped ac signal from the cell can handle up to 1.6 A of DC generated photocurrent. The monochromatic light power is monitored and measured simultaneous with the cell photocurrent signal using a NIST-calibrated sandwich Si/Ge photodetector through the beam splitter. The monochromatic light is chopped with a mechanical chopper at a nominal frequency of 43 Hz and the cell-generated signal is detected by a lock-in amplifier. Figure 2 shows the optical power of the monochromatic light beam at the sample location using a 150 W xenon (Xe) source, a 250 W quartz tungsten halogen (QTH), and a combination of the two (dual source) used in our apparatus for input into the monochromator. In the spectral range of 300 nm to 710 nm, we use the Xe source due to its high and relatively constant output power. At wavelengths greater than 710 nm, the monochromator input light is automatically switched to the more stable and constant QTH light source to provide a smooth and spike-free optical power. The dotted green plot represents the effective monochromatic optical beam shined on the device under test (DUT).

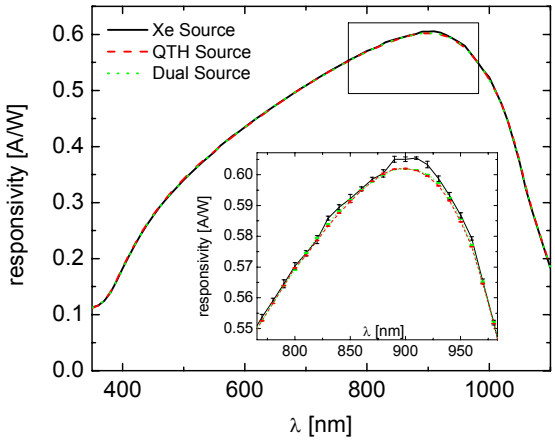

Figure 3 Spectral responsivity of a mono-Si reference solar cell measured at 25 °C in the underfilled illumination mode with our system without light bias (in dark).

Figure 3 shows the results of three measurements (Xe only light input, QTH only light input, and the dual source operation). In dual source mode, light source input is switched from Xe to QTH at the wavelength of 710 nm and above. Although all 3 plots show good agreement with each other, the zoomed-in plot shows that the use of the Xe source in the range of 750 nm to 950 nm introduces increased fluctuations and higher standard deviation in the measured data. This issue is circumvented by switching to the more stable QTH source

at all wavelengths above 710 nm. In these plots, the error bars represent the standard deviation of data at each wavelength as a result of 100 sequential measurements. Having established the advantageous aspects of the dual light source measurement, we now focus on the effect of light bias on solar cell spectral responsivity data. It is well known that some types of solar cells show a strong dependence on the level of light bias present during the measurement. The light bias should ideally be a broad spectrum light source, overfill the entire active device area and have intensities similar to the sun intensity (1000 W/m^2) at standard test conditions. Here, we discuss the effect of introducing two sources of light bias on the reference Si solar cell. Figure 4 shows the spectral responsivity of the cell under a light bias corresponding to a DC current of 50 mA (~ half sun intensity). The square symbols correspond to data taken under a 1 kW QTH DC light bias source at a monochromatic beam chopping frequency of 43 Hz. Significant sources of noise due to the QTH lamp (possibly the cooling fan) negatively affect the stability of the lock-in measurement, causing wide scatter in the data and large standard deviations. However, when a water-cooled white LED source is used as light bias, the noise is significantly suppressed and stable data is obtained at similar and even higher light bias current levels. These results highlight the importance of selecting stable biasing light sources.

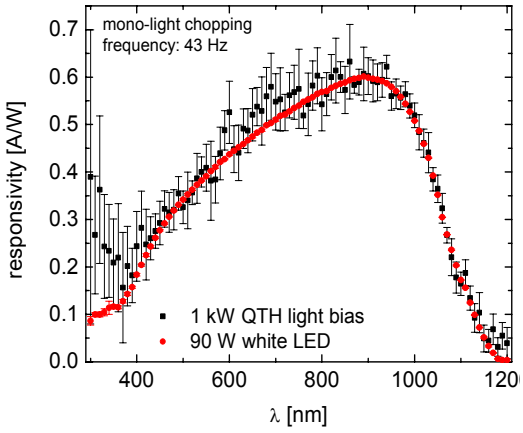

Figure 4 Spectral responsivity of the reference Si cell under a light bias DC current of 50 mA. The square symbols correspond to data taken under a 1 kW QTH DC light bias source at a monochromatic chopping frequency of 43 Hz.

Another way to mediate the high level of noise observed in the spectral response data using a QTH light bias source is to identify the frequency at which the noise is dominant and perform the measurements at chopping frequencies away from the noise source. In figure 5, we show that by setting the chopping frequency to 139 Hz instead of 43 Hz, the fluctuations are significantly reduced although not to the level of the white LED source. Further improvement is possible by employing a lock-in amplifier instrument with higher dynamic gain and better noise filtering. To surpass the disadvantage of lower dynamic gain for the lock-in amplifier used in this study a subroutine that allows an automatic averaging of acquired signal was introduced. This subroutine allows reaching signal to noise ratios of better than 10 000. The results using averaging and actual lock-in amplifier were perfectly comparable to results obtained with a lock-in amplifier with a higher dynamic range.

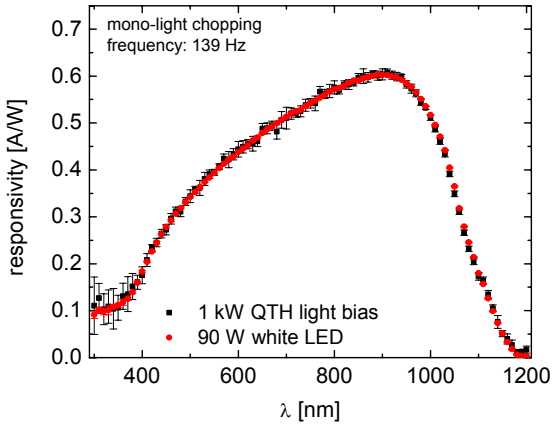

Figure 5 Spectral responsivity of the reference Si cell under a light bias DC current of 50 mA at monochromatic chopping frequency of 139 Hz. The QTH light biased data show a significant reduction in noise compared to the same measuremenent at 43 Hz (previous graph). The LED biased measurement looks similar to the previous measurement.

The spectral resolution was determined by finding the optical output from an HgAr calibrated lamp that has well defined spectral lines. Table 1 shows a direct comparison between the spectral positions of these lines found in the literature and the values determined using the system presented in this study. The values in Table 1 show that the system can determine the wavelength with accuracy better than 0.50 nm.

Table 1 Comparison between the wavelengths of theoretical spectral lines for HgAr calibration lamp and the values determined using our system

Wavelengths HgAr calibration lamp (nm)	**Wavelengths Measured (nm)**
404.66	405.00
435.84	436.00
546.07	545.50
576.96	576.50
579.07	579.00

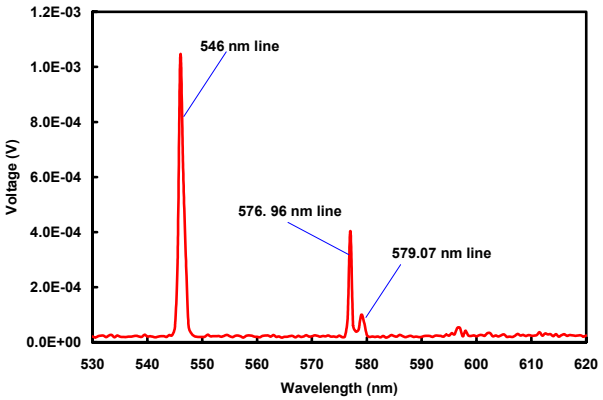

Figure 6 The spectrum obtained in the 530 – 600 nm region, showing the system can be tuned to obtain a spectral resolution better than 2.00 nm: 576.96 and 579.07 nm lines are clearly distinctive

The reflectance for each wavelength, $R_{d/s}(\lambda)$, is determined using the voltage measured by the corresponding (diffusive or specular) detector $V_{d/s}$, and the reference voltage measured by the reference detector, V_{ref}, using the equation:

$$R_{d/s}(\lambda) = m\frac{V_{d/s}}{V_{ref}} + n \qquad (1)$$

The coefficients *m* and *n* are found by a calibration process using NIST traceable reflectance standards. The functionality of the system, as shown in Figure 1, is not affected by adding an integrating sphere (IS) for diffuse measurements. The sample is close enough but not inside the integrating sphere. This positioning, in correlation with the small spot size relative to the IS port makes possible a diffuse measurement without removing the sample from the sample holder of the basic system. A good correlation was obtained between results acquired with the system presented here and measurements performed with a dedicated UV-IV spectrometer (Figure 7).

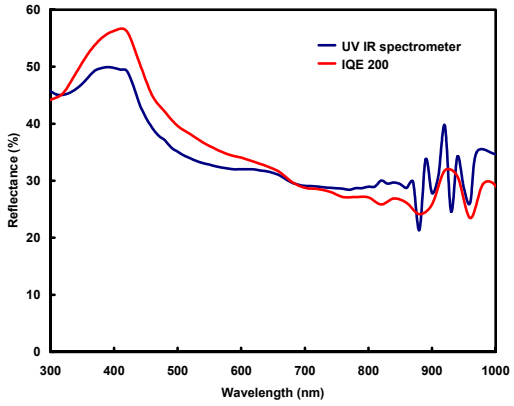

Figure 7 Comparison of reflectance measured by UV IR spectrometer and IQE 200 instrument. IQE 200 measurements were performed at lower spectral resolution (10 nm versus 20 nm).

III. Further Discussion

The capability of the system to discern between specular and diffuse component of reflectance, *Rs* and *Rd* respectively, is shown in Figure 8 that shows the results obtained on a mono crystalline Si textured sample. The capability of the system to measure both specular and diffuse components of reflectance is shown in Figure 8.

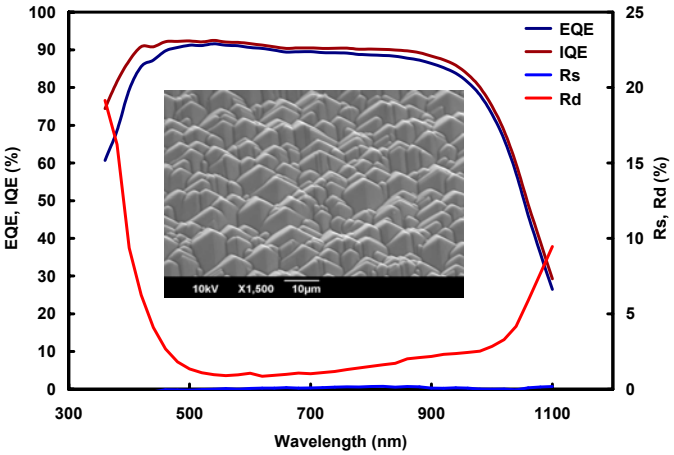

Figure 8 The specular and diffuse reflectance, external and internal quantum efficiency obtained for a mono-Si textured sample. A SEM image from surface roughness of the sample under test is shown in insert.

The capability of the system to perform both forward and reverse biasing, correlated with the capability to resolve low signal to noise cases was explored. Quantum efficiencies of the sample shown in the inset of figure 9 was measured in both reverse and forward bias voltages (V_{bias} =0.6 V). In reverse bias, the QE ratio of -0.6V/0V increases at longer wavelengths. This indicates that minority carrier collection from deep bulk area becomes more challenging with increasing wavelength. This becomes a significant loss in case of larger band gap materials. In the case of silicon, there is a difference of almost 60% in this ratio in wavelength range of 900-1100 nm, as indicated in Figure 9. In forward bias, the QE ratio of +0.6v/0v almost stays constant (Figure 9). In operation mode, the light induced current is made up of minority carriers which are swept by depletion layer electric field. On the other hand in forward bias, the majority carrier is supplied from an external source. In this case, diffusion current across the junction is a recombination current. Therefore, the majority carriers play the main role of conduction, which in this case would be holes in bulk p-Si area. Since they have to drift farther and have less mobility, they produce much smaller current which results in a very small light induced current, thereby a small QE. In the top graph, the absolute values of the ratio QE +0.6v/0v are shifted

by one unit, otherwise the absolute value of QE in +0.6v bias is close to zero.

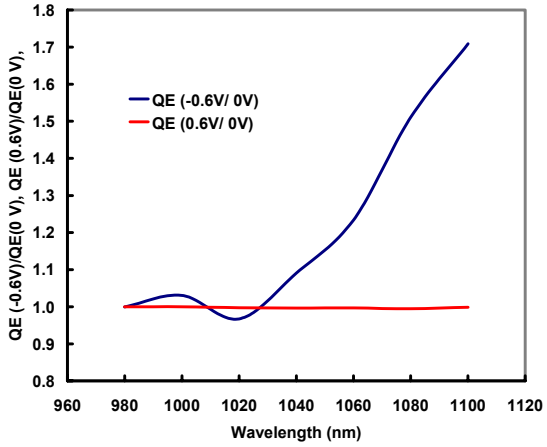

Figure 9 Forward versus reverse bias behavior for mono Si sample.

The electroluminescence (EL) measurements were performed for this study using the basic EL module shown in Figure 1. The integrating sphere assembly was replaced by an EL assembly consisting of: i) a Si/Ge bi-color detector; and ii) the focusing optics.

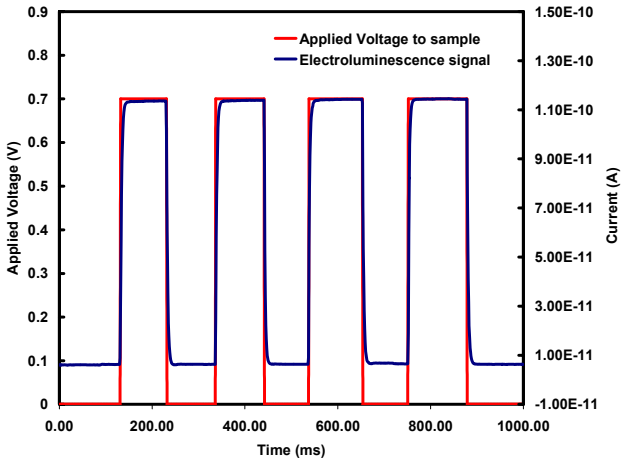

Figure 10 The experimental obtained with basic EL set-up. The EL output (red trace) clearly follows the applied voltage (blue trace).

This basic EL arrangement can be replaced by a camera or a spectrometer for EL spectral analysis. Figure 10 demonstrates that a basic EL arrangement can provide a ratio between on- and off- state signals better than 15:1. Small voltage excursions around 0.7 V are clearly detected by the system. The data shown in Figure 10 are raw data. t biasing two light sources equped with corresponding filter in order to saturate the lateral junctions.

VI. Conclusion

A system capable of performing multi-spectral IQE imaging is presented in this paper. The system is based on a tunable broad band optical source able to cover and extend the spectral domain between 300 nm and 1800 nm. The system is fully automated. The subroutine for computing J_{sc} directly from QE curves shows a good compatibility with values obtained from solar simulator based measurements. Maps of different parameters resulting from the spectral analysis can be obtained.

Acknowledgement

The authors wish to thank Keith Emery and Tom Moriarty from NREL for their for their constant theoretical and experimental support during elaborating of this paper.
We are very grateful to all our collaborators from NIST for their insightful inputs.

References

[1] D.M. Chapin, C.S. Fuller, G.L. Pearson, J. Appl. Phys. 25, 676 (1954). US Patent 2 780 765, 5 February 1957.

[2] J.L. Shay et al., "A simple measurement of absolute solar-cell efficiency" Journal of *Applied . Physics* 48, 1977, pp. 4this study853-4855.

[3] J. Metzdorf "Calibration of solar cells.1: The differential Spectral Responsivity Method", *Applied Optics* 26,1701, 1987.

[4] K. Emery "Organic PV Testing and Certification", *Organic Photovoltaics Summit,* Boston. October , 2009.

[5] A. Luque et al., "*Handbook of Photovoltaic Science and Engineering*", Wiley, pp. 702-713, 2005.

[6] E.F.Zalewski, The NBS photodetector spectral response calibration transfer program, Natl. Bur. Stand. (U.S.), Spec. Publ.250-17 pp. 45,1988.

[7] V.Shrotriya, et al. "Measurement and Characterization of Organic Solar Cells**"** *Adv. Funct. Mater.* 2006, *16*, 2016–2023

[8] G. Siefer et al., "External quantum efficiency measurements of germanium bottom Subcells: measurement artifacts and correction procedures" *IEEE 35th Photovoltaic Specialists Conference*, pp 704 – 707, 2010.

[9] R. Ciocan et al., *IEEE 35th Photovoltaic Specialists Conference*, pp 1675 – 1677, 2010.

.